
Facets for Art Gallery Problems

Sándor P. Fekete · Stephan Friedrichs ·
Alexander Kröller · Christiane Schmidt

Abstract The ART GALLERY PROBLEM (AGP) asks for placing a minimum number of stationary guards in a polygonal region P , such that all points in P are guarded. The problem is known to be NP-hard, and its inherent continuous structure (with both the set of points that need to be guarded and the set of points that can be used for guarding being uncountably infinite) makes it difficult to apply a straightforward formulation as an Integer Linear Program. We use an iterative primal-dual relaxation approach for solving AGP instances to optimality. At each stage, a pair of LP relaxations for a finite candidate subset of primal covering and dual packing constraints and variables is considered; these correspond to possible guard positions and points that are to be guarded.

Particularly useful are cutting planes for eliminating fractional solutions. We identify two classes of facets, based on EDGE COVER and SET COVER (SC) inequalities. Solving the separation problem for the latter is NP-complete, but exploiting the underlying geometric structure, we show that large subclasses of fractional SC solutions cannot occur for the AGP. This allows us to separate the relevant subset of facets in polynomial time. We also characterize all facets for finite AGP relaxations with coefficients in $\{0, 1, 2\}$.

Alexander Kröller was partially supported by DFG project Kunst!, KR 3133/1-1. Research was conducted while Stephan Friedrichs and Christiane Schmidt were affiliated with TU Braunschweig. Christiane Schmidt is supported by the Israeli Centers of Research Excellence (I-CORE) program (Center No. 4/11).

Sándor P. Fekete / Alexander Kröller
Technische Universität Braunschweig
Institut für Betriebssysteme und Rechnerverbund
E-mail: {s.fekete, a.kroeller}@tu-bs.de

Stephan Friedrichs
Max Planck Institute for Informatics, Saarbrücken, Germany
E-mail: sfriedri@mpi-inf.mpg.de

Christiane Schmidt
The Rachel and Selim Benin School of Computer Science and Engineering
The Hebrew University of Jerusalem
E-mail: cschmidt@cs.huji.ac.il

Finally, we demonstrate the practical usefulness of our approach. Our cutting plane technique yields a significant improvement in terms of speed and solution quality due to considerably reduced integrality gaps as compared to the approach by Kröller et al. [12].

Keywords Art Gallery Problem · geometric optimization · algorithm engineering · solving NP-hard problem instances to optimality · art gallery polytope · set cover polytope · facets · cutting planes

1 Introduction

The ART GALLERY PROBLEM (AGP) is one of the classical problems of geometric optimization: given a polygonal region P with n vertices, find as few stationary guards as possible, such that any point of the region is visible by at least one of the guards. As first proven by Chvátal [5] and then shown by Fisk [10] in a beautiful and concise proof (which is highlighted in the shortest chapter in “Proofs from THE BOOK” [1]), $\lfloor \frac{n}{3} \rfloor$ guards are sometimes necessary and always sufficient when P is a simple polygon. Worst-case bounds of this type are summarized under the name “Art-Gallery-type theorems”, and used as a metaphor even for unrelated problems; see O’Rourke [14] for an early overview, and Urrutia [17] for a more recent survey.

Algorithmically, the AGP is closely related to the SET COVER (SC) problem: All points in P have to be covered by star-shaped subregions of P . The AGP is NP-hard, even for a simply connected polygonal region P [13]. However, the SC problem has no underlying geometry, and it is well known that geometric variants of problems may be easier to solve or approximate than their discrete, graph-theoretic counterparts, so it is natural to explore ways to exploit the geometric nature of the AGP. But the AGP is far from being easily discretized, as both the set to be covered (all points in P) as well as the covering family (all star-shaped subregions around some point of P) usually are uncountably infinite.

It is natural to consider more discrete versions of the AGP. Ghosh [11] showed that restricting possible guard positions to the n vertices, i. e., the AGP with vertex guards, allows an $O(\log n)$ -approximation algorithm of complexity $O(n^5)$; conversely, Eidenbenz et al. [9] showed that for a region with holes, finding an optimal set of vertex guards is at least as hard as SC, so there is little hope of achieving a better approximation guarantee than $\Omega(\log n)$. While these results provide tight bounds in terms of approximation, they do by no means close the book on the arguably most important aspect of mathematical optimization: combining structural insights with powerful mathematical tools in order to achieve provably optimal solutions for instances of interesting size. Moreover, even a star-shaped polygon may require a large number of vertex guards, so general AGP instances may have significantly better solutions than the considerably simpler discretized version with vertex guards.

1.1 Solving AGP Instances

Computing optimal solutions for general AGP instances is not only relevant from a theoretical point of view, but has also gained in practical importance in the context of modeling, mapping and surveying complex environments, such as in the fields of architecture or robotics and even medicine, which are seeking to exploit the ever-improving capabilities of computer vision and laser scanning. Amit, Mitchell and Packer [2] have considered purely combinatorial primal and dual heuristics for general AGP instances. Only very recently have researchers begun to combine methods from integer linear programming with non-discrete geometry in order to obtain optimal solutions. As we have shown in [12], it is possible to combine an iterative primal-dual relaxation approach with structures from computational geometry in order to solve AGP instances with unrestricted guard positions; this approach is based on considering a sequence of primal and dual subproblems, each with a finite number of primal variables (corresponding to guard positions) and a finite number of dual variables (corresponding to “witness” positions).

Couto et al. [7, 8, 6] used a similar approach for the AGP with vertex guards. Tozoni et al. [16] proposed an algorithm that computes lower and upper bounds for the AGP, based on computing finite set-cover instances with the help of a state-of-the-art IP solver. To generate a lower bound, a finite set of witness candidates is chosen and a restricted AGP is solved, in which only the witnesses have to be covered. For this, it suffices to extract a finite set of potential guard positions from the visibility arrangement of the witness set in order to ensure optimality. Similarly, finite sets of potential witness positions for a given finite guard set can be extracted from the visibility arrangement of the guards. This allows it to compute upper and lower bounds for the optimal AGP value by solving discrete set cover instances. The algorithm of [16] iterates between generating tighter lower and upper bounds by refining the witness and guard candidate sets along the iterations. It stops when lower and upper bounds coincide. Although no theoretical convergence has been established, in tests, the approach is able to yield optimal solutions for a large variety of instance classes, even for polygons with up to a thousand vertices.

An approach presented in [12] considers a similar primal-dual scheme, but focuses on the linear relaxation of the primal guard cover, whose dual is the witness packing problem. This forms the basis of integer solutions and the approach presented in this paper; more details are described in Section 3. Furthermore, we have collaborated with the authors of [7, 8, 6, 16] and produced a video [4] that highlights and illustrates the approaches to the AGP, and also demonstrates its relevance for practical applications.

1.2 Set Cover

Also important for the work on the AGP is the discrete and finite problem of covering a given set of objects by an inexpensive collection of subsets. This is

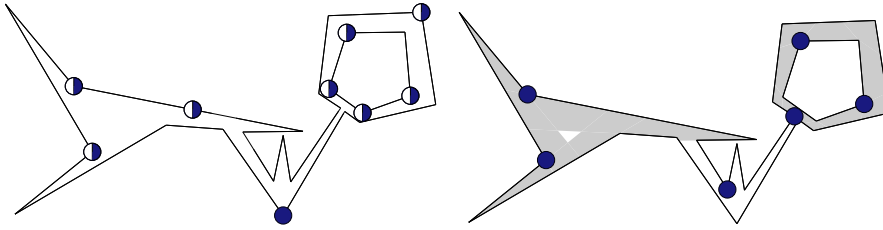


Figure 1 An optimal fractional solution of value 5 without (left) and an optimal integer solution of value 6 with cutting planes (right). Circles show guards, fill-in indicates fractional amount. Cutting planes enforce at least two guards in the left and three in the right area, both marked in gray.

known as the SET COVER PROBLEM (SC), which has enjoyed a considerable amount of attention. Highly relevant for the purposes of this paper is the work by Balas and Ng [3] on the discrete SC polytope, which describes all its facets with coefficients in $\{0, 1, 2\}$.

1.3 Our Results

In this paper, we extend and deepen our recent work [12] on iterative primal-dual relaxations, by proving a number of polyhedral properties of the resulting AGP polytopes and integrating them into modified versions of the algorithm presented in [12]. We provide the first study of the art gallery polytope and give a full characterization of all its facets with coefficients in $\{0, 1, 2\}$.

Remarkably, we are able to exploit geometry to prove that only a very restricted family of facets of the general SC polytope will typically have to be used as cutting planes for removing fractional variables. Instead, we are able to prove that many fractional solutions only occur in intermittent SC subproblems; thus, they simply vanish when new guards or witnesses are introduced. This saves us the trouble of solving an NP-complete separation problem. Computational results illustrate greatly reduced integrality gaps for a wide variety of benchmark instances, as well as reduced solution times. Details are as follows. Related SC results are described by Balas et al. [3].

- We provide two variants of our primal-dual framework for solving the AGP. Both aim at producing binary solutions, one integrates an IP in the primal phase and both greatly benefit from our cutting planes. Our algorithms also serve as benchmark for the cutting plane approach in our experiments.
- We show how to employ cutting planes for an iterative primal-dual framework for solving the AGP. This is interesting in itself, as it provides an approach to tackling optimization problems with infinitely many constraints and variables. The particular challenge is to identify constraints that remain valid for any choice of infinitely many possible primal and dual variables, as we are not solving one particular IP, but an iteratively refined sequence.

- Based on a geometric study of the involved SC constraints, we characterize all facets of involved AGP polytopes that have coefficients in $\{0, 1, 2\}$. In the SC setting, these facets are capable of cutting off fractional solutions, but the separation problem is NP-complete. We use geometry to prove that only some of these facets are able to cut off fractional solutions in an AGP setting under reasonable assumptions, allowing us to solve the separation problem in polynomial time.
- We provide a class of facets based on EDGE COVER (EC) constraints.
- We demonstrate the practical usefulness of our results by showing greatly improved solution speed and quality for a wide array of large benchmarks.

2 Preliminaries

We consider a polygonal region P with n vertices that may have holes, i. e., that does not have to be simply connected. For a point $p \in P$, we denote by $\mathcal{V}(p)$ the *visibility polygon* of p in P , i. e., the set of all $q \in P$, such that the straight-line connection \overline{pq} lies completely in P . P is *star-shaped* if $P = \mathcal{V}(p)$ for some $p \in P$. The set of all such points is the *kernel* of P , denoted by $\text{kernel}(P)$. For a set $S \subseteq P$, $\mathcal{V}(S) := \cup_{p \in S} \mathcal{V}(p)$.

A set $C \subseteq P$ is a *guard cover* of P , if $\mathcal{V}(C) = P$. The AGP asks for a guard cover of minimum cardinality c ; this is the same as covering P by a minimum number of star-shaped sub-regions of P . Note that Chvátal’s Watchman Theorem [5] guarantees $c \leq \lfloor \frac{n}{3} \rfloor$. For simplicity, we abbreviate $x(G) := \sum_{g \in G} x_g$, for any vector x .

3 Mathematical-Programming Formulation and LP-Based Solution Procedure

In order to keep this work self-contained, we briefly recapitulate our previously published [12] LP formulations of the AGP as well as how to use them to obtain fractional optimal Art Gallery solutions. Then we motivate the necessity to integrate cutting planes to cut off those fractional solutions in order to obtain binary ones. Furthermore, we specify requirements for cutting planes, allowing us to seamlessly integrate them in our framework.

Let P be a polygon and $G, W \subseteq P$ sets of points for possible guard locations and *witnesses*, i. e., points to be guarded, respectively. We assume $W \subseteq \mathcal{V}(G)$, which is easily guaranteed by initially including all vertices of P in G . The AGP that only requires covering W exclusively using guards in G can be

formulated as an IP denoted by $\text{AGP}(G, W)$:

$$\min \sum_{g \in G} x_g \quad (1)$$

$$\text{s. t.} \quad \sum_{g \in G \cap \mathcal{V}(w)} x_g \geq 1 \quad \forall w \in W \quad (2)$$

$$x_g \in \{0, 1\} \quad \forall g \in G, \quad (3)$$

where the original AGP is $\text{AGP}(P, P)$. Chvátal's Watchman Theorem [5] guarantees that only a finite number of variables in $\text{AGP}(P, P)$ are non-zero, but it still has uncountably many variables and constraints, so it cannot be solved directly. Thus we consider finite $G, W \subset P$ and iteratively solve $\text{AGP}(G, W)$ while adding points to G and W . For dual separation and to generate lower bounds, we require the LP relaxation $\text{AGR}(G, W)$ obtained by relaxing the integrality constraint (3) to:

$$0 \leq x_g \leq 1 \quad \forall g \in G. \quad (4)$$

The dual of $\text{AGR}(G, W)$ is

$$\max \sum_{w \in W} y_w \quad (5)$$

$$\text{s. t.} \quad \sum_{w \in W \cap \mathcal{V}(g)} y_w \leq 1 \quad \forall g \in G \quad (6)$$

$$0 \leq y_w \leq 1 \quad \forall w \in W. \quad (7)$$

The algorithms based on this formulation and the following argumentation are presented in pseudocode in Section 4 (Algorithms 1 and 2).

The relation between a solution of $\text{AGR}(G, W)$ and $\text{AGR}(P, P)$ is not obvious, see Figure 2 for the following argumentation. In [12], we show that $\text{AGR}(P, P)$ can be solved optimally for many problem instances by using finite G and W . The procedure uses primal/dual separation (i. e., cutting planes and column generation) to connect $\text{AGR}(G, W)$ to $\text{AGR}(P, P)$:

For some finite sets G and W , we solve $\text{AGR}(G, W)$ using the simplex method. This produces an optimal primal solution x^* and dual solution y^* with objective value z^* . The primal is a minimum covering of W by the guards in G , the dual a maximum packing of witnesses in W , such that each guard in G sees at most one of them. We analyze x^* and y^* as follows:

1. If there exists a point $w \in P \setminus W$ with $x^*(G \cap \mathcal{V}(w)) < 1$, then w corresponds to an inequality of $\text{AGR}(P, P)$ that is violated by x^* . The new witness w is added to W , and the LP is re-solved. If such a point w cannot be found, x^* is optimal for $\text{AGR}(G, P)$, and z^* is an upper bound for $\text{AGR}(P, P)$.
2. If there exists a point $g \in P \setminus G$ with $y^*(W \cap \mathcal{V}(g)) > 1$, then it corresponds to a violated dual inequality of $\text{AGR}(P, P)$. We create the LP column for g and re-solve the LP. If such a g does not exist, y^* is an optimal dual solution for $\text{AGR}(P, W)$ and z^* is a lower bound for $\text{AGR}(P, P)$.

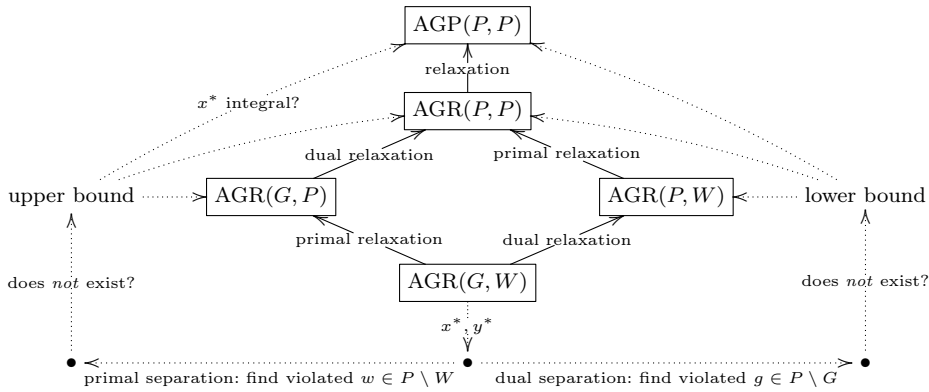


Figure 2 The AGP and its relaxations for $G, W \subseteq P$. Dotted arrows represent which conclusions may be drawn from the primal and dual solutions x^* and y^* .

Both separation problems can be solved efficiently using the overlay of the visibility polygons of all points $g \in G$ with $x_g^* > 0$ (for the primal case) and all $w \in W$ with $y_w^* > 0$ (for the dual case), which decomposes P into a planar arrangement of bounded complexity.

Should the upper and the lower bound meet, we have an optimal solution of $\text{AGR}(P, P)$, but $\text{AGR}(P, P)$ is the LP relaxation of $\text{AGP}(P, P)$, so its optimal solution may contain fractional guard values [12], compare Figure 1. At this point, it is possible to solve $\text{AGP}(G, P)$ using primal separation only, which produces binary upper bounds; but they do not necessarily match the lower bounds, which are still obtained using the relaxation. This scenario can prevent our procedure from terminating, even if it found an optimal Art Gallery solution, because it might be unable to prove its optimality. Algorithm 2 in Section 4 explores that approach.

In the remainder of this paper, we explore the use of cutting planes to cut off large classes of fractional solutions obtained by a procedure like the one described above, increasing lower bounds and enhancing integrality. Let α be such a cutting plane. Recall that $\text{AGP}(P, P)$ has an infinite number of both variables and constraints. That means that it is not enough for α to be feasible for $\text{AGP}(G, W)$ for the current iteration's finite sets G and W ; α must remain feasible in all future iterations of our algorithm. Formally, feasibility for $\text{AGP}(G, W)$ is insufficient; instead, we require α not to cut off any $x \in \{0, 1\}^{G'}$ for an arbitrary $P \supseteq G' \supseteq G$, such that x is feasible for $\text{AGP}(G', P)$. An LP with a set A of such additional constraints is denoted by $\text{AGR}(G, W, A)$, its IP counterpart by $\text{AGP}(G, W, A)$. Note that $\text{AGP}(G, P)$ and $\text{AGP}(G, P, A)$ have the same set of feasible solutions. By $\text{AGP}(G, W)$, we sometimes denote the set of its feasible solutions rather than the IP itself, as in $\text{conv}(\text{AGP}(G, W))$. See Section 4 for LP- and IP-based algorithms using the framework presented in this section.

```

Input: Polygon  $P$ 
1:  $G \leftarrow W \leftarrow$  all vertices of  $P$ 
2:  $A \leftarrow \emptyset$ 
3: (lowerBound, upperBound)  $\leftarrow (1, \infty)$ 

4: repeat
5:   repeat
6:      $(x^*, y^*) \leftarrow$  optimize AGR( $G, W, A$ )
7:      $W \leftarrow W \cup$  run primal separation
8:      $A \leftarrow A \cup$  separate cuts
9:     if separation failed and  $x^*$  is integral then
10:       upperBound  $\leftarrow$  min(upperBound, objective value of  $x^*$ )
11:     end if
12:   until separation failed or lowerBound = upperBound
13:   repeat
14:      $(x^*, y^*) \leftarrow$  optimize AGR( $G, W, A$ )
15:      $G \leftarrow G \cup$  run dual separation
16:      $A \leftarrow A \cup$  separate cuts
17:     if separation failed then
18:       lowerBound  $\leftarrow$  max(lowerBound,  $\lceil$ objective value of  $y^*$  $\rceil$ )
19:     end if
20:   until separation failed or lowerBound = upperBound
21: until lowerBound = upperBound or time limit reached

```

Algorithm 1 The LP mode algorithm only solves LPs.

4 Algorithms

The algorithm of Kröller et al. [12] produces fractional solutions of the AGP. We present two modifications, Algorithms 1 and 2, focused on obtaining binary solutions.

Our first modification, used in both algorithms, is that we do not run primal and dual separation, compare Section 3, in every iteration. Instead, we repeatedly run primal (dual) separation until a primally (dually) feasible solution has been obtained and then switch to running dual (primal) separation until a feasible dual (primal) solution has been found, and so on. We call these phases *primal (dual) phases* and repeat an alternating sequence of them, until primally and dually feasible solutions with matching bounds have been found.

4.1 LP Mode

Algorithm 1 relies on cutting planes to cut off fractional solutions that are feasible for AGR(G, P), but not AGP(G, P). Those cutting planes are constraints in the primal LP, and variables in the dual. This means that they have two effects: They enhance the integrality of acquired solutions and they increase the lower bound.

The issue with this approach is that we are not guaranteed to find a binary solution, because we might not have a cutting plane available which is able to cut off the current primal solution.


```

Input: Polygon  $P$ 
1:  $G \leftarrow W \leftarrow$  all vertices of  $P$ 
2:  $A \leftarrow \emptyset$ 
3: (lowerBound, upperBound)  $\leftarrow (1, \infty)$ 

4: repeat
5:   repeat
6:      $x^* \leftarrow$  optimize AGP( $G, W, A$ )
7:      $W \leftarrow W \cup$  run primal separation
8:     if separation failed then
9:       upperBound  $\leftarrow$  min(upperBound, objective value of  $x^*$ )
10:    end if
11:   until separation failed or lowerBound = upperBound
12:   repeat
13:      $(x^*, y^*) \leftarrow$  optimize AGR( $G, W, A$ )
14:      $G \leftarrow G \cup$  run dual separation
15:      $A \leftarrow A \cup$  separate cuts
16:     if separation failed then
17:       lowerBound  $\leftarrow$  max(lowerBound,  $\lceil$ objective value of  $y^*$  $\rceil$ )
18:    end if
19:   until separation failed or lowerBound = upperBound
20: until lowerBound = upperBound or time limit reached

```

Algorithm 2 The IP mode algorithm has one difference to Algorithm 1: It solves IPs in the primal separation phase, thus only producing binary upper bounds.

4.2 IP Mode

The typical approach of eliminating fractional solutions in linear optimization is to employ an integer program (IP). In Algorithm 2, we solve AGP(G, W, A) for finite $G, W \subset P$ and iteratively apply primal separation to the result, which produces feasible binary solutions.

Unfortunately, this procedure does not necessarily find optimal solutions of AGP(P, P), because it does not generate new guard positions: For generating guards we need a dual solution, which an IP cannot provide. To counter that, we use the dual phase of Algorithm 1 where we solve the LP AGR(G, W, A). This step is supported by cutting planes, which help increase the lower bound and thus reducing the integrality gap.

Note that Algorithm 2 is not guaranteed to terminate, because an optimal fractional and an optimal binary solution may require different guard locations [12]. This effect is weakened, but not completely suppressed by the use of cutting planes. The impact is that there is an integrality gap between the upper and the lower bounds, which can be large.

5 Set Cover Facets

For finite sets of guards and witnesses $G, W \subset P$, AGP(G, W) is an SC polytope. This motivates the investigation of SC-based facets. In this section, we discuss a family of facets inspired by Balas et al. [3] and show that their separation, while NP-complete in the SC setting, can, under reasonable assumptions,

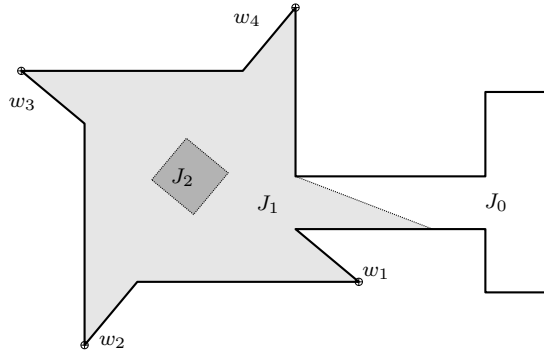


Figure 3 Polygon and witness selection $S = \{w_1, w_2, w_3, w_4\}$. Guards located in J_2 can cover all of S , and those in J_1 some part of it, while those in J_0 cover none of S .

be solved in polynomial time when exploiting the underlying geometry of the AGP. Additionally, we present a complete list of all AGP facets only using coefficients in $\{0, 1, 2\}$.

5.1 A Family of Facets

Let P be a polygon and $G, W \subset P$ finite sets of guard and witness positions. Consider a finite non-empty subset $\emptyset \subset S \subseteq W$ of witness positions; the overlay of visibility regions of S is called α_S . It implies the partition $P = J_0 \dot{\cup} J_1 \dot{\cup} J_2$, see Figure 3. This is the geometry that is analogous to what Balas and Ng [3] did for the SC polytope.

1. $J_2 := \{g \in P \mid S \subseteq \mathcal{V}(g)\}$, the set of points in P covering all of S .
2. $J_0 := \{g \in P \mid \mathcal{V}(g) \cap S = \emptyset\}$, the set of positions in P that see none of S .
3. $J_1 := P \setminus (J_2 \cup J_0)$ the set of positions in P that cover a non-trivial subset of S .

Every feasible solution of the AGP has to cover S . Thus, it takes one guard in J_2 , or at least two guards in J_1 to cover S . For any G , this induces the following constraint (8); for the sake of simplicity, we will also refer to this by α_S .

$$\sum_{g \in J_2 \cap G} 2x_g + \sum_{g \in J_1 \cap G} x_g \geq 2 \quad (8)$$

In the context of our iterative algorithm, it is important to represent α_S independently from G . This is achieved by storing the visibility overlay of the witnesses in S , which implicitly makes the regions J_0 , J_1 and J_2 available. Any guard $g \in J_i$ in current or future iterations simply gets the coefficient i .

Sufficient coverage of S is necessary for sufficient coverage of P , so (8) is valid for any $x \in \{0, 1\}^G$ that is feasible for $\text{AGP}(G, P)$, thus fulfilling our requirement of remaining feasible in future iterations. However, covering S

may require more than two guards in J_1 , so (8) does not always provide a supporting hyperplane of $\text{conv}(\text{AGP}(G, W))$.

When choosing a single witness $S = \{w\}$, we obtain $J_2 = \mathcal{V}(w)$, $J_1 = \emptyset$ and $J_0 = P \setminus \mathcal{V}(w)$. The resulting constraint is Inequality (2), the witness-induced constraint of w , multiplied by two. For a choice of S with two witnesses, $S = \{w_1, w_2\}$, constraint (8) yields the sum of the witness-induced constraints of w_1 and w_2 . Thus, we consider $|S| \geq 3$ in the remainder of this section.

In order to show when (8) defines a facet of $\text{conv}(\text{AGP}(G, W))$, we first need to apply a result of [3] to the AGP setting.

Lemma 1 *Let P be a polygon and $G, W \subset P$ finite sets of guard and witness positions. Then $\text{conv}(\text{AGP}(G, W))$ is full-dimensional, if and only if*

$$\forall w \in W : |\mathcal{V}(w) \cap G| \geq 2 \quad (9)$$

Proof. We start by proving necessity. If every witness is seen by at least two guards, the $|G|$ vectors $x^i = \mathbf{1} - e_i$ are linearly independent and feasible solutions of $\text{AGP}(G, W)$, so $\text{conv}(\text{AGP}(G, W))$ is full-dimensional.

Now we consider sufficiency. If $\mathcal{V}(w) \cap G = \emptyset$ for some $w \in W$, there is no feasible solution at all; if $\mathcal{V}(w) \cap G = \{g\}$, there is none with $x_g = 0$, so there cannot be more than $|G| - 1$ linearly independent solutions, and $\text{conv}(\text{AGP}(G, W))$ is not full-dimensional. \square

We require some terminology adapted from [3]. Two guards $g_1, g_2 \in J_1$ are a *2-cover* of α_S , if $S \subseteq \mathcal{V}(g_1) \cup \mathcal{V}(g_2)$. The *2-cover graph* of G and α_S is the graph with nodes in $J_1 \cap G$ and an edge between g_1 and g_2 if and only if g_1, g_2 are a 2-cover of α_S . In addition, we have $T(g) = \{w \in \mathcal{V}(g) \cap W \mid \mathcal{V}(w) \cap G \cap (J_0 \setminus \{g\}) = \emptyset\}$.

Theorem 1 *Given a polygon P and finite $G, W \subset P$, let $\text{conv}(\text{AGP}(G, W))$ be full-dimensional and let α_S be as defined in (8), such that S is maximal, i. e., there is no $w \in W \setminus S$ with $\mathcal{V}(w) \subseteq \mathcal{V}(S)$. Then the constraint induced by α_S defines a facet of $\text{conv}(\text{AGP}(G, W))$, if and only if:*

1. *Every component of the 2-cover graph of α_S and G has an odd cycle.*
2. *For every $g \in J_0 \cap G$ such that $T(g) \neq \emptyset$ there exists either*
 - (a) *some $g' \in J_2 \cap G$ such that $T(g) \subseteq \mathcal{V}(g')$;*
 - (b) *some pair $g', g'' \in J_1 \cap G$ such that $T(g) \cup S \subseteq \mathcal{V}(g') \cup \mathcal{V}(g'')$.*

Proof. G and W are finite, so $\text{AGP}(G, W)$ is an instance of SC with universe W and subsets G , while $\text{conv}(\text{AGP}(G, W))$ describes a full-dimensional SC polytope.

Our claim follows from Theorem 2.6 of Balas et al. [3], because the conditions as well as the notion of 2-cover graphs and T are equivalent. The only difference is that we need to intersect J_i with G in order to obtain finite sets, as our J_i is a region in P , while that of Balas et al. naturally is a finite set of variables. \square

5.2 Geometric Properties of α_S

It is easy to construct SC instances for any choice of $|S| \geq 3$, such that the SC version of α_S cuts off a fractional solution [3]. Finding α_S in the SC setting is NP-complete, see below. But in the following, we show that in an AGP setting, only α_S with $|S| = 3$ actually plays a role in cutting off fractional solutions under reasonable assumptions, allowing us to separate it in polynomial time.

Lemma 2 *Let P be a polygon, $G, W \subset P$ finite sets of guard and witness positions and $\emptyset \subset S \subseteq W$. If every guard in $J_1 \cap G$ belongs to some 2-cover of α_S and S is minimal for G , i. e., there is no proper subset $T \subset S$ such that α_T and α_S induce the same constraint for G , the matrix of $\text{AGP}(G, S)$ contains a permutation of the full circulant of order $k = |S|$, which is*

$$C_k^{k-1} = \begin{pmatrix} 0 & 1 & \cdots & 1 \\ 1 & 0 & \ddots & \vdots \\ \vdots & \ddots & \ddots & 1 \\ 1 & \cdots & 1 & 0 \end{pmatrix} \in \{0, 1\}^{k \times k}. \quad (10)$$

Proof. As G and W are finite, $\text{conv}(\text{AGP}(G, W))$ is an SC polytope with universe W and subsets G . Then, as above, the claim follows from Balas et al. or, or more accurately, from Theorem 3.1 of [3]: Our definition of S being minimal for G complies with the definition of a minimal C -equivalent subset in [3]; the notion of matrix $A_S^{J_1}$ corresponds to our $\text{AGP}(J_1 \cap G, S)$, i. e., a submatrix of $\text{AGP}(G, S)$. \square

Lemma 2 holds, because the 2-cover property holds if and only if no guard's coefficient in α_S can be reduced without turning Inequality (8) invalid [3]. As S is minimal, removing w from S must increase coefficients, i. e., reclassify a guard $g \in J_1 \cap G$ to J_2 . So $\mathcal{V}(g) \cap S = S \setminus \{w\}$. Such a guard exists for every $w \in S$.

Lemma 2 also states that separating α_S is equivalent to finding permutations of C_k^{k-1} in the LP matrix of $\text{AGR}(G, W)$. It is possible to reduce a simple graph's adjacency matrix to a polygon with guards G and witnesses W , such that $\text{AGR}(G, W)$ contains a permutation of C_k^{k-1} if and only if the graph contains a clique of size k or higher: Introduce a guard and a witness for each of the graph's vertices, place all of them into a convex polygon, and add a hole between a guard and a witness if they represent the same vertex or if the two vertices are not connected. Hence, the separation problem is NP-complete.

In the following, we examine when the separation of α_S is useful for our iterative algorithm. As α_S is represented by one or several permutations of C_k^{k-1} , we need to introduce the notion of a polygon corresponding to C_k^{k-1} . This allows us to examine the underlying geometry of α_S in the AGP.

Definition 1 (Full Circulant Polygon) A polygon P along with $G(P) = \{g_1, \dots, g_k\} \subset P$ and $W(P) = \{w_1, \dots, w_k\} \subset P$ for $3 \leq k \in \mathbb{N}$ is called *Full*

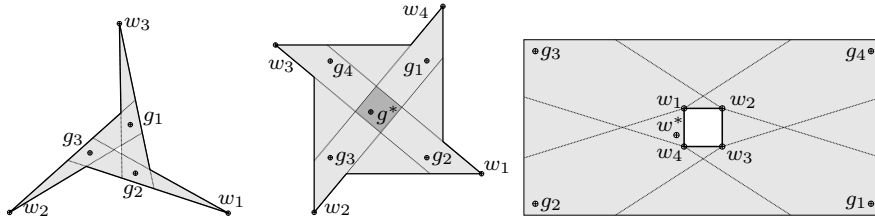


Figure 4 P_3^2 (left) and two attempts for P_4^3 (middle and right). In the left case, Inequality (8) enforces using two guards instead of three $\frac{1}{2}$ -guards.

The first attempt for P_4^3 (middle) is star-shaped; here a cutting plane would cut off the intermediate fractional solution of four $\frac{1}{3}$ -guards, but as soon as g^* is found, the fractional solution is replaced by a binary one with just one guard, with or without cutting plane.

Finally, the second attempt for P_4^3 (right) is not star-shaped, but again, there is no need for a cutting plane to cut off the fractional solution of four $\frac{1}{3}$ -guards: w^* is only covered by $\frac{2}{3}$, so w^* is separated by our algorithm and then enforces the use of at least two guards in the next iteration; again, with or without cutting plane.

Circulant Polygon, or P_k^{k-1} , if

$$\forall 1 \leq i \leq k : \quad \mathcal{V}(g_i) \cap W(P) = W(P) \setminus \{w_i\} \quad (11)$$

$$\forall w \in P : \quad |\mathcal{V}(w) \cap G(P)| \geq k - 1 \quad (12)$$

We may refer to $G(P)$ and $W(P)$ by just G and W , respectively.

Note that in P_k^{k-1} the full circulant C_k^{k-1} completely describes the visibility relations between G and W . This implies that the optimal solution of $\text{AGR}(G, W)$ is $\frac{1}{k-1} \cdot \mathbf{1}$, with cost $\frac{k}{k-1}$. It is feasible for $\text{AGR}(G, P_k^{k-1})$ by Property (12), as any point $w \in P_k^{k-1}$ is covered by at least $(k-1) \cdot \frac{1}{k-1} = 1$.

Figure 4 captures construction attempts for models of C_k^{k-1} . P_3^2 exists; however, as we prove in Theorem 2, the polygons for $k \geq 4$ are either star-shaped or not full circulant. If they are star-shaped, the optimal solution is to place one guard within the kernel. If they are not full circulant polygons, the optimal solution of $\text{AGR}(G, W)$ is infeasible for $\text{AGR}(G, P)$ and the current fractional solution is intermittent, i. e., cut off in the next iteration. Both cases eliminate the need for a cutting plane, and we may avoid the NP-complete separation problem by restricting separation to $k = 3$.

In the following we prove that P_k^{k-1} is star-shaped for $k \geq 4$. We start with Lemma 3, which shows that any pair of guards in G is sufficient to cover P_k^{k-1} .

Lemma 3 *Let P_k^{k-1} be a full circulant polygon. Then P_k^{k-1} is the union of the visibility polygons of any pair of guards in G ($P_k^{k-1} = \{g_1, \dots, g_k\}$):*

$$\forall 1 \leq i < j \leq k : \quad P_k^{k-1} = \mathcal{V}(g_i) \cup \mathcal{V}(g_j) \quad (13)$$

Proof. Suppose P_k^{k-1} is a full circulant polygon, but $P_k^{k-1} \neq \mathcal{V}(g_i) \cup \mathcal{V}(g_j)$ for $1 \leq i < j \leq k$. Then there exists some $w \in P_k^{k-1}$ with $g_i \notin \mathcal{V}(w)$, as well as

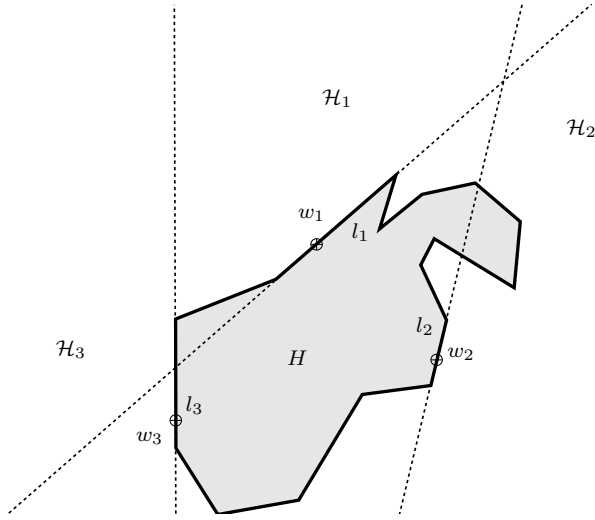


Figure 5 A hole H in P_k^{k-1} with $\mathcal{H}_1 \cap \mathcal{H}_2 \cap \mathcal{H}_3 = \emptyset$. There are $k-1$ guards in \mathcal{H}_1 and in \mathcal{H}_2 , so there must be $k-2$ in their intersection. This only leaves 2 guards for \mathcal{H}_3 .

$g_j \notin \mathcal{V}(w)$, implying that $|\mathcal{V}(w) \cap G| \leq k-2$, a contradiction to Property (12) of Definition 1. \square

The next step is Lemma 4, which drastically restricts the possible structure of P_k^{k-1} .

Lemma 4 *Let P_k^{k-1} be a full circulant polygon with $G(P_k^{k-1}) = \{g_1, \dots, g_k\}$. Suppose $k \geq 4$. Then P_k^{k-1} has no holes.*

Proof. Refer to Figure 5. Suppose P_k^{k-1} has a hole H . Each edge l_i of H induces a half-space \mathcal{H}_i . There are three such edges l_1, l_2, l_3 , such that $\mathcal{H}_1 \cap \mathcal{H}_2 \cap \mathcal{H}_3 = \emptyset$, for otherwise the outside of H would be convex by Helly's Theorem. Let w_i denote a point in the interior of l_i .

In order for w_1 to fulfill (12), at least $k-1$ of the guards in G must be located in $\mathcal{V}(w_1) \subseteq \mathcal{H}_1$. Analogously, there must be $k-1$ guards in \mathcal{H}_2 . Covering w_1 and w_2 with a total of k guards is only possible if at least $k-2$ guards of G are located in the intersection of the two half-spaces: $|\mathcal{H}_1 \cap \mathcal{H}_2 \cap G| \geq k-2$. If there are only $k' < k-2$ guards in $\mathcal{H}_1 \cap \mathcal{H}_2$, it takes $(k-1) - k'$ additional guards in $\mathcal{H}_1 \setminus \mathcal{H}_2$ to cover w_1 and in $\mathcal{H}_2 \setminus \mathcal{H}_1$ to cover w_2 , resulting in a total of $k' + 2(k-1-k') = 2k - (k'+2) > k$ guards, a contradiction.

As $\mathcal{H}_1 \cap \mathcal{H}_2 \cap \mathcal{H}_3 = \emptyset$, there can be at most 2 guards in $\mathcal{V}(w_3) \subseteq \mathcal{H}_3$, which violates Property (12) for $k \geq 4$, a contradiction. \square

As shown in Figure 6, $k \geq 4$ is tight: a triangle with a concentric triangular hole is an example of P_3^2 , with guards in the outside corners and witnesses on the inside edges.

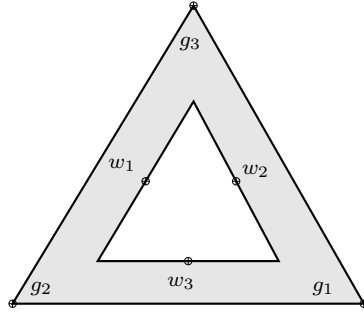


Figure 6 P_3^2 , a possible AG interpretation of C_3^2 with a hole. It proves that the bound of $k \geq 4$ in Lemma 4 is tight.

We require one final technical lemma before proceeding to the main theorem, Theorem 2.

Lemma 5 *Consider two disjoint non-empty convex polygons, described as the intersection of half-spaces: $P_1 = \bigcap_{i=1, \dots, n} \mathcal{H}_i$ and $P_2 = \bigcap_{i=n+1, \dots, n+m} \mathcal{H}_i$. Then some \mathcal{H}_i , $1 \leq i \leq n + m$ separates P_1 and P_2 .*

Proof. $n + m \leq 2$ is trivial, so consider $n + m \geq 3$. Because of $P_1 \cap P_2 = \bigcap_{i=1, \dots, n+m} \mathcal{H}_i = \emptyset$, Helly's Theorem applied to the two-dimensional convex half-spaces \mathcal{H}_i implies the existence of three half-spaces $\mathcal{H}_i, \mathcal{H}_j$, and \mathcal{H}_k , $i < j < k$, with $\mathcal{H}_i \cap \mathcal{H}_j \cap \mathcal{H}_k = \emptyset$. Without loss of generality, we assume $i = 1$, $j = 2$ and $k = n + 1$, which provides

$$\underbrace{\mathcal{H}_1 \cap \mathcal{H}_2}_{\supseteq P_1} \cap \underbrace{\mathcal{H}_{n+1}}_{\supseteq P_2} = \emptyset, \tag{14}$$

so it follows that $P_1 \cap \mathcal{H}_{n+1} = \emptyset$ with $P_2 \subseteq \mathcal{H}_{n+1}$ by construction, and \mathcal{H}_{n+1} is the half-space whose existence is the claim. \square

Now all preliminaries for the main theorem of the section are met and we can proceed to show Theorem 2, which claims that full circulant polygons are star-shaped for $k \geq 4$.

Theorem 2 *A full circulant polygon P_k^{k-1} with $k \geq 4$ is star-shaped.*

Proof. Refer to Figure 7. Let P_k^{k-1} with $k \geq 4$ be a full circulant polygon. The guards in $G = G(P_k^{k-1})$ must be covered by a total of $k - 1$ guards, i. e., they must also fulfill (12), so each guard can see at least $k - 2$ others. Without loss of generality, let g_1 and g_2 denote two guards in each other's field of view.

Now consider $P_{12} = \mathcal{V}(g_1) \cap \mathcal{V}(g_2) \subseteq P_k^{k-1}$, the subset of P_k^{k-1} seen by both g_1 and g_2 . It is star-shaped, because g_1 and g_2 are in its kernel, which we denote by K . The rest of P_k^{k-1} , i. e., $P_k^{k-1} \setminus P_{12}$, consists of two types of areas:

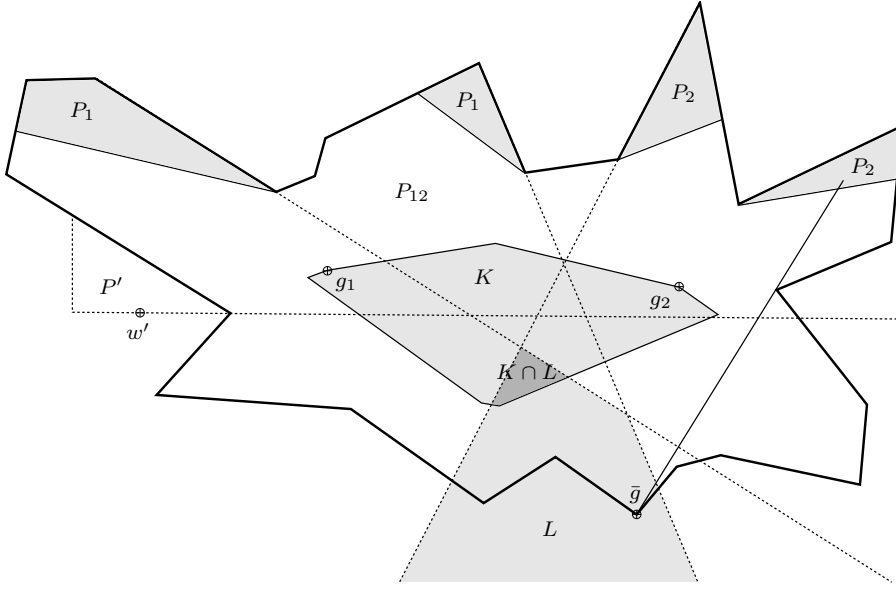


Figure 7 P_k^{k-1} with guards g_1 and g_2 . P_1 and P_2 are the gray areas at the top. P_1 is seen by g_1 but not by g_2 ; an analogous property holds for P_2 . The rest of P_k^{k-1} is P_{12} , a star-shaped polygon entirely seen by both g_1 and g_2 , K is its kernel. L is the area whose view into $P_1 \cup P_2$ is not blocked by any edge of P_k^{k-1} that coincides with $P_1 \cup P_2$. It contains all of g_3, \dots, g_k .
If P' would be added to P_k^{k-1} , K would be cut off below the dashed line containing w' and $K \cap L = \emptyset$. But then no point in L , including g_3, \dots, g_k , could see w' , a contradiction to the property of P_k^{k-1} requiring $k - 1$ guards to see any of its points.

1. $P_1 = P_k^{k-1} \setminus (P_{12} \cup \mathcal{V}(g_2))$, points visible from g_1 , but not from g_2 .
2. $P_2 = P_k^{k-1} \setminus (P_{12} \cup \mathcal{V}(g_1))$, points visible from g_2 , but not from g_1 .

Together, g_1 and g_2 cover every $w \in P_k^{k-1}$, because $P_k^{k-1} = \mathcal{V}(g_1) \cup \mathcal{V}(g_2)$ due to Lemma 3. Thus, $P_k^{k-1} = P_{12} \dot{\cup} P_1 \dot{\cup} P_2$.

We now examine which guards can see what part of P_{12} , P_1 and P_2 . For that, we classify three types of edges. *Gray* edges are those edges of P_k^{k-1} that coincide with P_1 or P_2 , *white* edges denote the other edges of P_k^{k-1} . Finally, edges of P_{12} not part of P_k^{k-1} that separate $P_1 \cup P_2$ from P_{12} are referred to as *white-gray* edges. Note that white-gray edges do not block the view of any guard in P_k^{k-1} , because they are merely edges of the auxiliary polygon P_{12} . K is the intersection of all half-spaces induced by white or white-gray edges, because a star's kernel is the intersection of all half-spaces induced by its edges.

All points able to cover all of $P_1 \cup P_2$ must be contained in

$$\begin{aligned}
 L &= \{g \in \mathbb{R}^2 \mid \text{no gray edge blocks } g\text{'s view into } P_1 \text{ or } P_2\} \\
 &= \bigcap_{e \text{ is gray edge}} \text{Half-space induced by } e.
 \end{aligned} \tag{15}$$

Some points in L may be located outside of P_k^{k-1} , and even those points of L inside of P_k^{k-1} may not be able to see all of $P_1 \cup P_2$, due to white edges blocking their view. \bar{g} in Figure 7 is an example for this case: it cannot see the rightmost part of P_2 . However, $L \neq \emptyset$, because $g_3, \dots, g_k \in L \cap P_k^{k-1}$. Every $g_i \in G$ with $3 \leq i \leq k$ is able to see all of $P_1 \cup P_2$: g_i can see all of P_1 , because g_2, g_i are a 2-cover of P_k^{k-1} ; g_i can entirely see P_2 , because g_1, g_i are also a 2-cover by Lemma 3.

The remaining part of the proof involves two steps. First, we argue that any point in $K \cap L$ can see all of P_k^{k-1} ; then we show that $K \cap L \neq \emptyset$, i. e., that P_k^{k-1} is star-shaped. For the first step, assume there exists some $g \in K \cap L$. Now g has the following properties:

1. $g \in P_k^{k-1}$, because $K \subseteq P_k^{k-1}$.
2. g can see all of P_{12} by definition of K , which includes the interior of P_{12} , all white and all white-gray edges.
3. Because P_k^{k-1} has no holes by Lemma 4, g 's view on the white-gray edges is not blocked; and due to $g \in L$, there is nothing left that can block g 's view into $P_1 \cup P_2$.

So $g \in \text{kernel}(P_k^{k-1})$, provided that $K \cap L \neq \emptyset$; we show the latter as follows.

K and L are two-dimensional polyhedra, each of their edges is a facet. Suppose their intersection is empty; then by Lemma 5, there must be a facet of one of them that separates them from each other. We consider three cases, because K has two types of edges and L has one:

1. The facet is a facet of K , induced by a white edge e . Now consider a point w in the interior of e . w is seen by g_1 and g_2 , but not by any of the points g_3, \dots, g_k , because $g_3, \dots, g_k \in L$, and e induces a facet separating K from L . Due to $k \geq 4$, this makes $|\mathcal{V}(w) \cap G| \geq k - 1$, i. e., (12), impossible and thus contradicts the requirement of P_k^{k-1} being a full circulant polygon. This would be the case in Figure 7, if P_k^{k-1} had the extension P' , which would cut off the lower part of K and thus separate K from L . However, then only g_1 and g_2 but none of g_3, \dots, g_k could see w' , which violates (12).
2. The facet is a facet of K , induced by a white-gray edge e . As e is a white-gray edge, there is a part of P_1 or P_2 adjacent to e . This part cannot be seen from any point in L , because the facet induced by e is a facet of K and separates K from L by assumption, and because P_k^{k-1} has no holes by Lemma 4. However, $g_3, \dots, g_k \in L$ not being able to see P_1 or P_2 contradicts (12).
3. The facet is a facet of L . This means that there is some gray edge e corresponding to that facet. A point w in e 's interior is not seen by g_1 or g_2 , because the facet separates K from L . So s is not seen by more than $k - 2$ guards, and thus violates (12).

All cases lead to contradiction, and thus $K \cap L \neq \emptyset$. Therefore, P_k^{k-1} has a non-empty kernel, and is star-shaped for $k \geq 4$, as claimed. \square

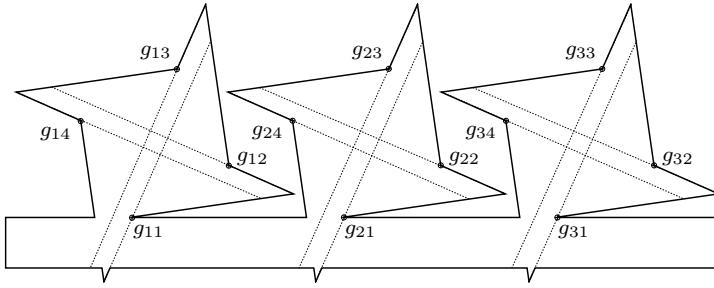


Figure 8 Three instances of P_4^3 embedded into a larger polygon. Setting all guards to $\frac{1}{3}$ is feasible and optimal, even though no guard is placed in any of the P_4^3 kernels.

Theorem 2 does not rule out situations in which P_k^{k-1} , for $k \geq 4$ is part of a larger polygon, as shown in Figure 8. This example has no integrality gap; placing at least five copies of P_4^3 around an appropriate central subpolygon with a hole can actually create one. However, such cases are much harder to come by, making the $k \geq 4$ facets a lot less useful for cutting off fractional solutions.

Theorem 2 does, however, provide a very useful separation heuristic. As the separation problem is NP-complete for unlimited k , but solvable in polynomial time for a fixed k , it is clear that k must be limited in a practical algorithm. Theorem 2 justifies choosing $k = 3$ from a theoretical point of view, by stating that the underlying geometry for $k > 3$ is star-shaped, i. e., allows placing one non-fractional guard in its kernel, see Figure 4. As we show in Section 7, this can also be validated in an experimental setting.

5.3 All Art Gallery Facets with Coefficients $\{0, 1, 2\}$

For finite $G, W \subset P$, $\text{AGP}(G, W)$ is also an SC instance. Balas and Ng identified all SC facets with coefficients in $\{0, 1, 2\}$ [3]; so we present all AGP facets with coefficients $\{0, 1, 2\}$. This includes three trivial facet classes, (16) – (18), which are unable to cut off fractional solutions of $\text{AGR}(G, W)$. The only non-trivial facet in this inventory is the one of type α_S described above.

$$x_g \geq 0 \tag{16}$$

is a facet of a full-dimensional $\text{conv}(\text{AGP}(G, W))$, and only if $|\mathcal{V}(w) \cap G \setminus \{g\}| \geq 2$ for all $w \in W$, i. e., if every witness sees at least two guards other than g .

A second type of AGP facet is the upper bound of one for every guard value. It is a facet of every full-dimensional $\text{conv}(\text{AGP}(G, W))$ [3]:

$$x_g \leq 1 \tag{17}$$

The third and last trivial AGP facet with coefficients in $\{0, 1, 2\}$ is

$$\sum_{g \in \mathcal{V}(w) \cap G} x_g \geq 1 \tag{18}$$

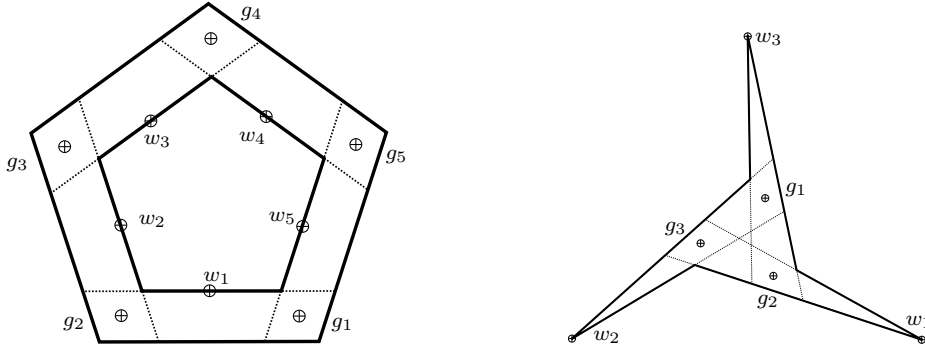


Figure 9 Two situations, in which no guard exists that can see more than two witnesses. On the left, assigning $g_1 = \dots = g_5 = \frac{1}{2}$ results in an optimal fractional solution of $\frac{5}{2}$, compare [12]. Applying (19) yields $g_1 + \dots + g_5 \geq \frac{5+1}{2} = 3$ and cuts off this fractional solution. On the right, the optimal fractional solution is $g_1 = g_2 = g_3 = \frac{1}{2}$. (19) provides the constraint $g_1 + g_2 + g_3 \geq \frac{3+1}{2} = 2$, which cuts off that fractional solution as well.

This simply is the constraint induced by the witness $w \in W$, which enforces sufficient coverage of w . It is facet defining and only if two conditions hold: First, there must not be any witness $w' \in W$ with $\mathcal{V}(w') \cap G \subset \mathcal{V}(w) \cap G$. Otherwise, the coverage of w would be implied by that of w' . Second, for any guard $g \in G \setminus \mathcal{V}(w)$, there exists some other guard $g' \in \mathcal{V}(w) \cap G$ that can see all of $\{w' \in \mathcal{V}(g) \cap W \mid \bar{g} \notin \mathcal{V}(w'), \forall \bar{g} \in G \setminus (\mathcal{V}(w) \cup \{g\})\}$, compare [3].

The fourth, and the only non-trivial, AGP facet with coefficients in $\{0, 1, 2\}$ is the facet of type α_S presented in Inequality (8) and Theorem 1, which is thoroughly analyzed above.

6 Edge Cover Facets

Solving $\text{AGR}(G, W)$ for finite $G, W \subset P$, such that no guard can see more than two witnesses is equivalent to solving fractional edge cover (EC) on the graph with nodes W , an edge between $v \neq w \in W$ for each $g \in G$ with $\mathcal{V}(g) \cap W = \{v, w\}$, and a loop for each $g \in G$ with $\mathcal{V}(g) \cap W = \{w\}$. The fractional EC polytope is known to be half-integral [15], which can be exploited to show that fractional solutions always form odd-length cycles of $\frac{1}{2}$ -guards.

In the conclusions of [12], we proposed a class of valid inequalities motivated by this. The idea is to identify k witnesses $\bar{W} = \{w_1, \dots, w_k\}$, such that no point exists that can see more than two of them. Then at least $\lceil \frac{k}{2} \rceil$ binary guards are needed for covering \bar{W} . Two examples are shown in Figure 9.

$$\sum_{g \in \mathcal{V}(\bar{W}) \cap G} x_g \geq \left\lceil \frac{k}{2} \right\rceil \quad (19)$$

Obviously, for any choice of $P \supseteq G' \supseteq G$, (19) does not cut off any feasible solution $x \in \{0, 1\}^{G'}$ of $\text{AGP}(G', P)$, as long as no point in P exists that sees more than two of these witnesses. Hence, analogously to the SC cuts, a cut can be represented as visibility overlay $\alpha_{\overline{W}}$ and kept in future iterations once it has been identified.

It is not hard to show that these are facet defining under relatively mild conditions.

Theorem 3 *Let P be a polygon with finite sets of guard and witness positions $G, W \subset P$, such that $\text{conv}(\text{AGP}(G, W))$ is full-dimensional. Let $\overline{W} = \{w_1, \dots, w_k\} \subseteq W$ be an odd subset of $k \geq 3$ witnesses, such that*

1. *No guard sees more than two witnesses in \overline{W} .*
2. *If a guard sees two witnesses $w_i \neq w_j \in \overline{W}$, they are a successive pair, i. e., $i + 1 = j$ or $i = 1$ and $j = k$.*
3. *Each of the k successive pairs is seen by some $g \in G$.*
4. *No guard inside of $\mathcal{V}(\overline{W})$ sees a witness outside of \overline{W} .*

Then the constraint

$$\sum_{g \in \mathcal{V}(\overline{W}) \cap G} x_g \geq \left\lceil \frac{|\overline{W}|}{2} \right\rceil \quad (20)$$

is a facet of $\text{conv}(\text{AGP}(G, W))$.

Proof. As no guard sees more than two witnesses of \overline{W} , it is clear that it takes at least $\lceil \frac{k}{2} \rceil$ guards to cover \overline{W} .

It remains to be shown how to construct $n = |G|$ affinely independent solutions of $\text{AGP}(G, W)$. In order to do that, we separate the guards into three groups $G_1 \dot{\cup} G_2 \dot{\cup} G_3 = G$ with $|G_i| = n_i$:

1. G_1 is a set of one guard for each successive pair as in Condition 3.
2. G_2 contains all guards in $\mathcal{V}(\overline{W})$ that are not already part of G_1 :

$$G_2 = (\mathcal{V}(\overline{W}) \cap G) \setminus G_1 \quad (21)$$

3. G_3 holds the rest of the guards, which are outside of $\mathcal{V}(\overline{W})$:

$$G_3 = G \setminus \mathcal{V}(\overline{W}) \quad (22)$$

In the following, we describe a solution $x \in \{0, 1\}^G$ by $x = (x_{G_1}, x_{G_2}, x_{G_3})$, where $x_{G_i} \in \{0, 1\}^{G_i}$ denotes the vector $(x_{g_1}, \dots, x_{g_{n_i}})$ with $G_i = \{g_1, \dots, g_{n_i}\}$. The first set of n_1 solutions is

$$\begin{aligned} x^1 &= ((1, 0, 1, 0, \dots, 1, 0, 1), \quad \mathbf{0}, \quad \mathbf{1}) \\ x^2 &= ((1, 1, 0, 1, \dots, 0, 1, 0), \quad \mathbf{0}, \quad \mathbf{1}) \\ x^3 &= ((0, 1, 1, 0, \dots, 1, 0, 1), \quad \mathbf{0}, \quad \mathbf{1}) \\ &\vdots \\ x^{n_1} &= ((0, 1, 0, 1, \dots, 0, 1, 1), \quad \mathbf{0}, \quad \mathbf{1}), \end{aligned} \quad (23)$$

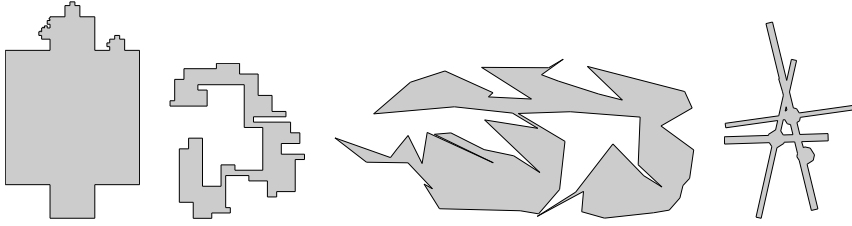


Figure 10 Small *von Koch*, *Orthogonal*, *Simple* and *Spike* test polygons.

which exists because of Condition 3 and the choice of G_1 . It fulfills (20) with equality because it uses $\lceil \frac{k}{2} \rceil$ guards, and it is feasible, because \overline{W} and $W \setminus \overline{W}$ are covered by construction and guards not in G_3 do not interfere with the coverage of witnesses in $W \setminus \overline{W}$.

The second set provides n_2 solutions by using the i -th unit vector as x_{G_2} .

$$x^i = (x', \quad e_i, \quad \mathbf{1}) \quad (24)$$

As every successive pair of witnesses is covered by some guard in G_1 , a choice of x' such that x^i fulfills (20) with equality is always possible.

The third and last set of n_3 solutions is constructed by subtracting e_i from $\mathbf{1}$ in the vector x_{G_3} :

$$x^i = ((1, 0, 1, 0, \dots, 1, 0, 1), \quad \mathbf{0}, \quad \mathbf{1} - e_i). \quad (25)$$

It fulfills (20) with equality. Setting one guard value to zero in G_3 is feasible because in a full-dimensional $\text{conv}(\text{AGP}(G, W))$, every witness is seen by at least two guards, compare Lemma 1.

All in all, we have $n_1 + n_2 + n_3 = n$ feasible, affinely independent solutions of $\text{AGP}(G, W)$ fulfilling (20) with equality, so (20) has dimension $n - 1$ and is a facet, as claimed. \square

7 Computational Experience

A variety of experiments on benchmark polygons demonstrates the usefulness of our cutting planes, as well as the appropriateness of our separation heuristic of using only $k = 3$ for the SC related facets from Section 5.

We test our cutting planes in two variations of our algorithm, IP and LP mode, i. e., Algorithms 2 and 1 from Section 4. An in-depth presentation of the results is conducted in Sections 7.1 and 7.2.

Just as in [12], we employed four different classes of benchmark polygons.

1. Random *von Koch* polygons are inspired by fractal Koch curves, see Figure 10, left.
2. Random floorplan-like *Orthogonal* polygons as in Figure 10, second polygon.

3. Random non-orthogonal *Simple* polygons as in Figure 10, third polygon.
4. Random *Spike* polygons (mostly with holes) as in Figure 10, fourth polygon.

Each polygon class was evaluated for different sizes $n \in \{60, 200, 500, 1000\}$, where n is the approximate number of vertices in a polygon.

Different combinations of cut separators were also employed. The EC-related cuts from Section 6 are referred to as *EC cuts*, while the SC-related cuts of Section 5 that rely on separating a maximum of $3 \leq k$ witnesses are denoted by *SC k cuts*. Note that for $3 \leq m \leq k$, *SC k cuts* also include all *SC m cuts*.

Whenever our algorithm separates cuts, it applies all configured cut separators and we test the following combinations: no cut separation at all, SC3 cuts only, SC4 cuts only, EC cuts only, and SC3 and EC cuts at the same time.

In total, we have two modes, five combinations of separators, four classes of polygons, and four polygon sizes; for each combination, we tested 10 different polygons. The experiments were run on 3.0 GHz Intel dual core PCs with 2 GB of memory, running 32 bit Debian 6.0.5 with Linux 2.6.32-686. Our algorithms were not parallelized, used version 4.0 of the ‘‘Computational Geometry Algorithms Library’’ (CGAL) and CPLEX 12.1. Each test run had a time limit of 600 s.

In the remaining part of this section, we refer to quartiles by Q_0, Q_1, Q_2, Q_3 and Q_4 . Q_1 is the first quartile, which is between the lowest 25% and the rest of the values. Q_2 is the second quartile or the median value and Q_3 , the third quartile, splits the upper 25% from the lower 75%. For the sake of simplicity, the minimum and the maximum are denoted by Q_0 and Q_4 , respectively.

7.1 IP Mode

The IP mode, Algorithm 2, is a variation of the one introduced in [12], which always determines binary solutions at the expense of not necessarily terminating due to the integrality gap. Our experiments confirm that the integrality gap is drastically reduced by our cutting planes.

In Figure 11 we present the relative gap over time for the five tested cut separator selections for the *von Koch*-type polygons with 1000 vertices. Figure 11(a) shows the relative gap over time without cut separation. After about 400 s, gaps are fixed between 0% and 6%, the median gap being 2%. When applying the EC separator (Figure 11(b)), 75% of the gaps drop to zero and the largest gap is 2%. Using the SC3 separator (Figure 11(c)) yields an even better result in terms of both speed and relative gap. All gaps are closed, many of them earlier than with the EC separator. Combining both, see Figure 11(d), yields a result comparable to using only SC3. Moving to the SC4 separator (Figure 11(e)) yields a weaker performance: computation times go up, and not all gaps reach 0% within the allotted time, because separation takes longer

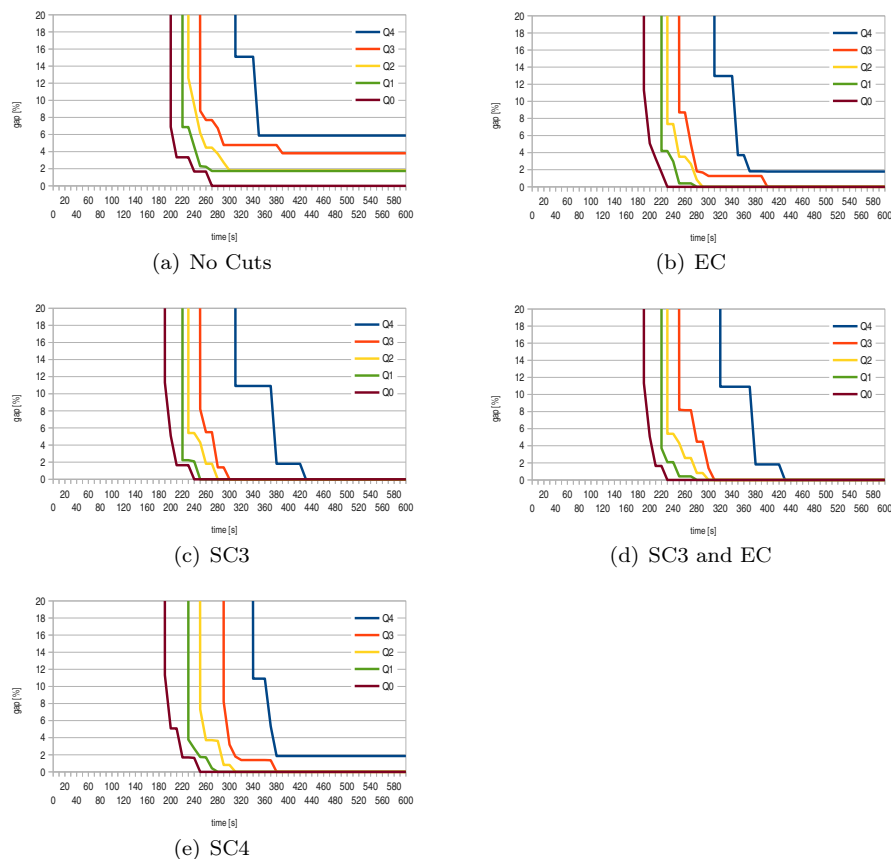


Figure 11 Relative gap over time in IP-mode for 1000-vertex *von Koch*-type polygons.

without improving the gap. This illustrates the practical consequences of Theorem 2.

The remaining test cases, i. e., the remaining polygon classes, confirm our interpretation. We briefly summarize only the deviating observations.

For the *Orthogonal*-type polygons with 1000 vertices in Figure 12, EC and SC3 separation yield an improvement over using no separation: The maximum relative gap drops and some gaps reach their 600s levels earlier. Joint application of SC3 and EC provides the best results. SC4 and SC3 separation only differ in the extreme cases of the minimum and the maximum relative gap.

The 1000-vertex *Simple* polygons, see Figure 13, allow a slight improvement of the relative gap with EC as well as SC3 separation; joint application yields the best results. A difference to the other experiments is that the SC4 separator performs slightly better than the SC3 separator – an isolated observation.

Our separators have no measurable impact on the *Spike*-type polygons, see Figure 14. Larger instances of this type of polygon take much time when

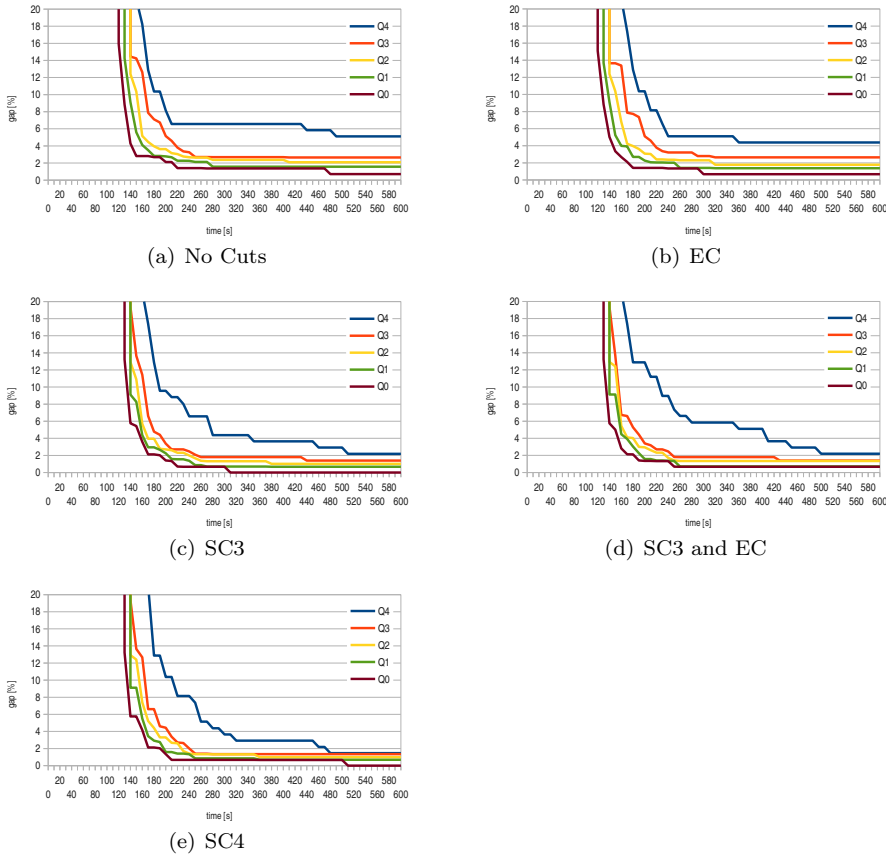


Figure 12 Relative gap over time in IP-mode for the 1000-vertex *Orthogonal*-type polygons.

solving the first couple of IPs, which means our separators are triggered late in the 600s time limit – or not at all.

7.2 LP Mode

Analogously to the IP mode, we test the separators in LP mode, i. e., Algorithm 1. The difference to Algorithm 2 is that in the primal phase, it solves the LP $\text{AGR}(G, W, A)$ instead of the IP. If a solution of $\text{AGR}(G, W, A)$ is feasible for $\text{AGR}(G, P, A)$ and if it happens to be binary, it is an upper bound, otherwise it is discarded and the primal phase is continued.

The challenge of the LP mode is to find a binary solution at all, because the algorithm might stick to fractional optimal solutions that are not handled by any cut separator. Instances unsolved because of this are considered to have

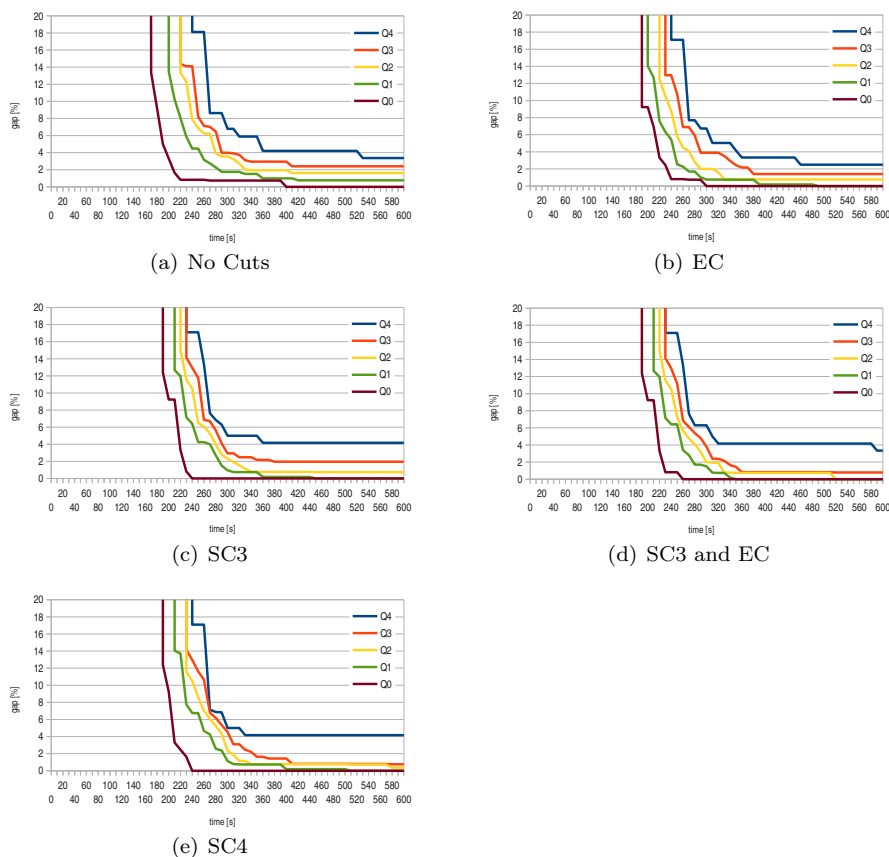


Figure 13 Relative gap over time in IP-mode for the 1000-vertex *Simple*-type polygons.

an infinite gap; they result in diagrams in which only the lower quartiles are visible.

Figures 15, 16, 17 and 18 show the relative gap over time diagrams for the 500-vertex *von Koch*, *Orthogonal* and *Simple*, as well as the 200-vertex *Spike* polygons.

For the *von Koch* polygons in Figure 15, the EC separator provides a slight improvement, the SC3 separator a stronger improvement; the best result is obtained when using both of them. SC4 separation is weaker than SC3 separation.

The EC separator does not improve the situation for the *Orthogonal* polygons, Figure 16, but the SC3 separator boosts solution percentage beyond 75%. Joint application of both separators results in even smaller gaps. SC4 cut separation yields mixed results: The median relative gap is larger, while the Q_3 gap is smaller but takes approximately 350s longer to reach its value. In addition, the Q_1 curve takes much longer to drop to zero as well.

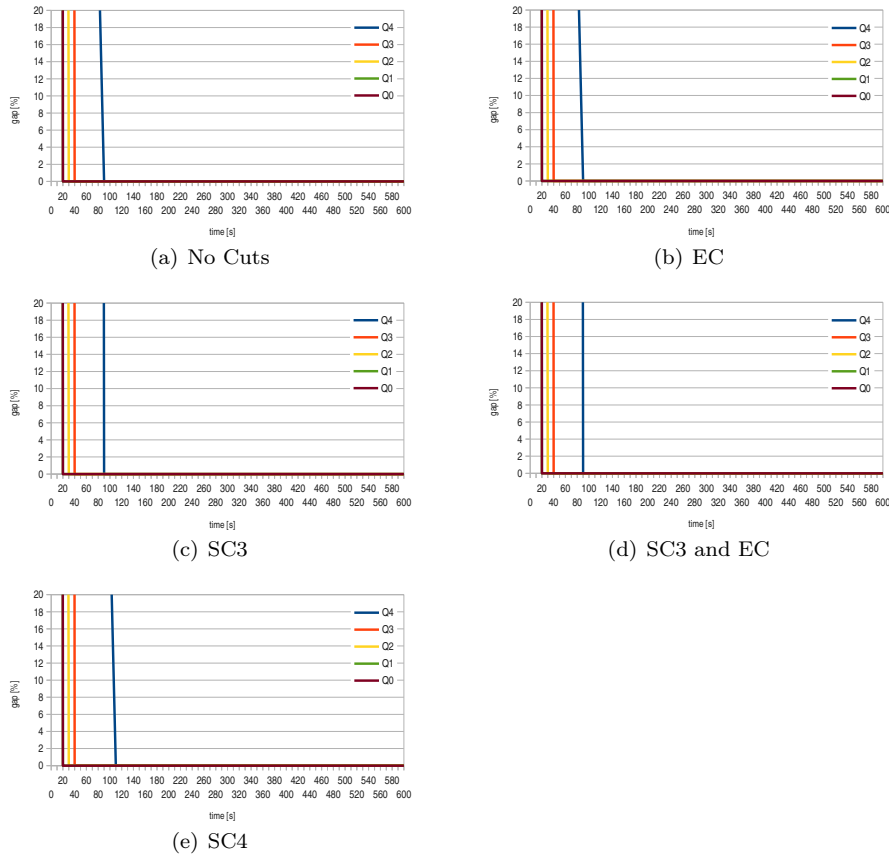


Figure 14 Relative gap over time in IP-mode for the 200-vertex *Spike*-type polygons.

The situation for the *Simple* polygons in Figure 17 is as follows. EC separation has no impact on the results, when applied alone as well as when used jointly. As above, SC3 separation is better than SC4 separation, it solves more instances.

EC cuts have no impact on the *Spike* polygons, Figure 18, but SC3 helps solving all of them instead of less than 25%. In this case, the SC4 separator is approximately 10s faster in the Q_1 , Q_2 and Q_3 quartiles and 30s for the maximum.

We present Table 1 that summarizes the solution percentage after 600s in LP mode as well as the median relative gap.

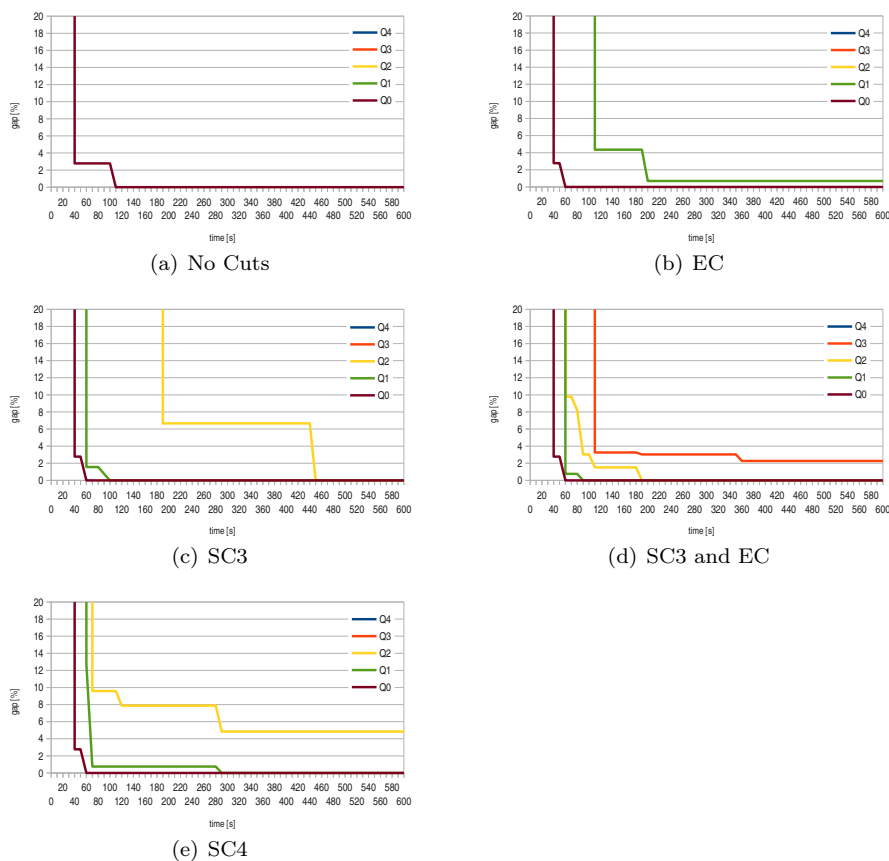


Figure 15 Relative gap over time in LP-mode for the 500-vertex *von Koch*-type polygons.

8 Conclusion

In this paper, we have shown how we can exploit both geometric properties and polyhedral methods of mathematical programming to solve a classical and natural, but highly challenging problem from computational geometry.

We have shown how to integrate cutting planes into linear programming formulations of the Art Gallery Problem (AGP), a linear program with a potentially infinite number of both variables and constraints. Additionally, we provided three trivial and two non-trivial facets of the AGP polytope based on SET COVER and EDGE COVER, including a complete list of all AGP facets with coefficients in $\{0, 1, 2\}$.

Furthermore, we have exploited the underlying geometric properties of the AGP to identify a subset of one of our facet classes, that

1. can be separated in polynomial time, although the general separation problem is NP-complete.

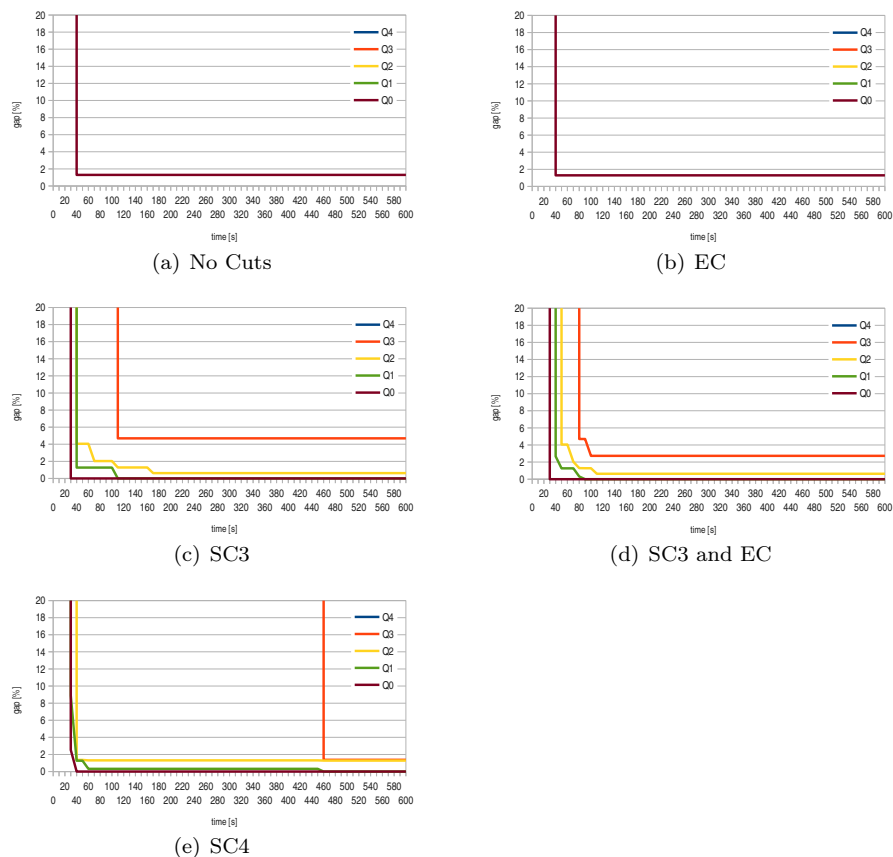


Figure 16 Relative gap over time in LP-mode for the 500-vertex *Orthogonal*-type polygons.

2. is theoretically justified by showing that geometry behind the cutting planes is star-shaped for the cases excluded in separation.
3. is justified by experimental data.

This promises to pave the way for a range of practical AGP applications that have to deal with additional real-life aspects. We are optimistic that our basic approach can also be used for other geometric optimization problems.

References

1. Aigner, M., Ziegler, G.M.: Proofs from THE BOOK (3. edition). Springer (2004)
2. Amit, Y., Mitchell, J.S.B., Packer, E.: Locating guards for visibility coverage of polygons. *International Journal of Computational Geometry and Applications* **20**(5), 601–630 (2010)
3. Balas, E., Ng, M.: On the set covering polytope: I. all the facets with coefficients in $\{0, 1, 2\}$. *Mathematical Programming* **43**(1), 57–69 (1989)

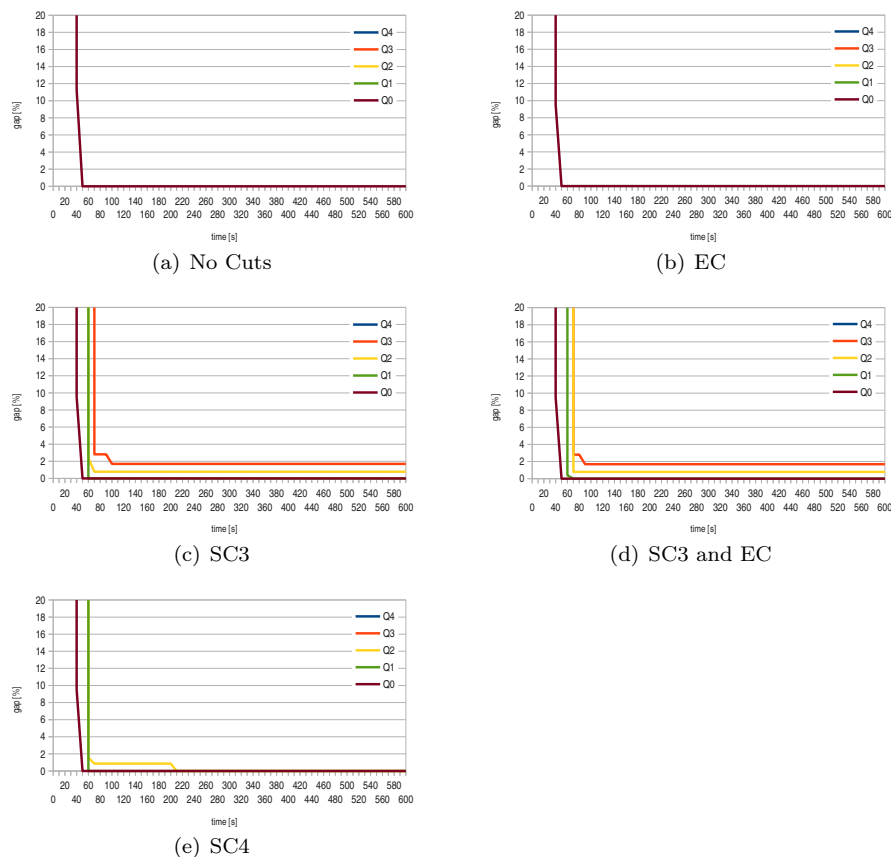


Figure 17 Relative gap over time in LP-mode for the 500-vertex *Simple*-type polygons.

4. Borrmann, D., de Rezende, P.J., de Souza, C.C., Fekete, S.P., Friedrichs, S., Kröller, A., Nüchter, A., Schmidt, C., Tozoni, D.C.: Point guards and point clouds: Solving general art gallery problems. In: Proc. 29th ACM Symposium on Computational Geometry (SoCG'13), pp. 347–348 (2013). Video available at <http://imaginary.org/film/point-guards-and-point-clouds-solving-general-art-gallery-problems>
5. Chvátal, V.: A combinatorial theorem in plane geometry. *Journal of Combinatorial Theory (B)* **18**, 39–41 (1975)
6. Couto, M.C., de Rezende, P.J., de Souza, C.C.: An exact algorithm for minimizing vertex guards on art galleries. *International Transactions in Operational Research* **18**, 425–448 (2011)
7. Couto, M.C., de Souza, C.C., de Rezende, P.J.: An exact and efficient algorithm for the orthogonal art gallery problem. In: SIBGRAPI '07: Proceedings of the XX Brazilian Symposium on Computer Graphics and Image Processing, pp. 87–94. IEEE Computer Society, Washington, DC, USA (2007)
8. Couto, M.C., de Souza, C.C., de Rezende, P.J.: Experimental evaluation of an exact algorithm for the orthogonal art gallery problem. In: WEA '08: 7th International Workshop on Experimental Algorithms, pp. 101–113 (2008)
9. Eidenbenz, S., Stamm, C., Widmayer, P.: Inapproximability results for guarding polygons and terrains. *Algorithmica* **31**(1), 79–113 (2001)

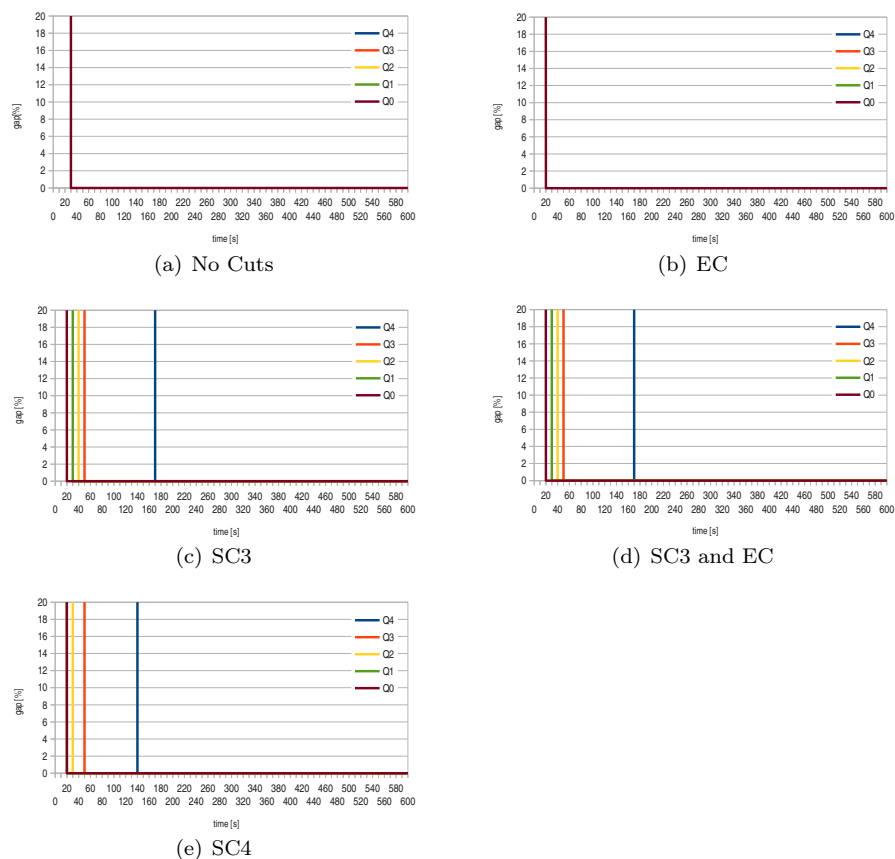


Figure 18 Relative gap over time in LP-mode for the 200-vertex *Spike*-type polygons.

10. Fisk, S.: A short proof of Chvátal's watchman theorem. *Journal of Combinatorial Theory, Series B* (3), 374 (1978)
11. Ghosh, S.K.: Approximation algorithms for art gallery problems in polygons and terrains. In: WALCOM, *LNCS*, vol. 5942, pp. 21–34. Springer (2010)
12. Kröller, A., Baumgartner, T., Fekete, S.P., Schmidt, C.: Exact solutions and bounds for general art gallery problems. *ACM Journal of Experimental Algorithmics* **17**(1), 2.3:2.1–2.3:2.23 (2012)
13. Lee, D.T., Lin, A.K.: Computational complexity of art gallery problems. *IEEE Transactions on Information Theory* **32**(2), 276–282 (1986)
14. O'Rourke, J.: *Art Gallery Theorems and Algorithms*. International Series of Monographs on Computer Science. Oxford University Press, New York, NY (1987)
15. Schrijver, A.: *Combinatorial Optimization - Polyhedra and Efficiency*. Springer (2003)
16. Tozoni, D.C., de Rezende, P.J., de Souza, C.C.: The quest for optimal solutions for the art gallery problem: a practical iterative algorithm. *Optimization Online* (2013). www.optimization-online.org/DB_HTML/2013/01/3734.htm
17. Urrutia, J.: Art gallery and illumination problems. In: J.R. Sack, J. Urrutia (eds.) *Handbook on Computational Geometry*, pp. 973–1026. Elsevier (2000)

Vertices	no cuts	EC	SC3	EC and SC3	SC4
von Koch					
60	90%, 0.0%	90%, 0.0%	100%, 0.0%	100%, 0.0%	100%, 0.0%
200	30%, 0.0%	20%, 0.0%	90%, 0.0%	90%, 0.0%	80%, 0.0%
500	20%, 1.4%	50%, 0.0%	60%, 0.0%	90%, 0.0%	70%, 0.0%
1000	0%, n/a	20%, 0.0%	60%, 0.0%	40%, 0.0%	30%, 0.0%
Orthogonal					
60	80%, 0.0%	80%, 0.0%	100%, 0.0%	100%, 0.0%	100%, 0.0%
200	40%, 7.5%	60%, 1.7%	90%, 0.0%	90%, 0.0%	90%, 0.0%
500	10%, 1.3%	10%, 1.3%	80%, 0.0%	90%, 0.0%	80%, 1.3%
1000	0%, n/a	0%, n/a	40%, 2.0%	40%, 2.1%	40%, 2.0%
Simple					
60	100%, 0.0%	100%, 0.0%	100%, 0.0%	100%, 0.0%	100%, 0.0%
200	40%, 3.5%	50%, 0.0%	100%, 0.0%	90%, 0.0%	100%, 0.0%
500	10%, 0.0%	10%, 0.0%	80%, 0.0%	80%, 0.0%	70%, 0.0%
1000	0%, n/a	0%, n/a	50%, 0.7%	50%, 0.0%	50%, 0.7%
Spike					
60	100%, 0.0%	100%, 0.0%	100%, 0.0%	100%, 0.0%	100%, 0.0%
200	10%, 0.0%	20%, 0.0%	100%, 0.0%	100%, 0.0%	100%, 0.0%
500	0%, n/a	0%, n/a	20%, 0.0%	20%, 0.0%	10%, 0.0%
1000	0%, n/a	0%, n/a	0%, n/a	0%, n/a	0%, n/a

Table 1 After 600 s, for each polygon/size combination and for every tested cut separator combination, this table shows for how many percent of the polygons a binary solution was found as well as their median relative gap.